Radial distribution functions and densities for the SPC/E, TIP4P and TIP5P models for liquid water and ices I_h, I_c, II, III, IV, V, VI, VII, VIII, IX, XI and XII†

Carlos Vega,* Carl McBride, Eduardo Sanz and Jose L. F. Abascal

Departamento de Química Física, Facultad de Ciencias Químicas, Universidad Complutense de Madrid, Ciudad Universitaria, 28040 Madrid, Spain

Monte Carlo computer simulation studies have been undertaken for virtually all of the ice phases as well as for liquid water for three of the most popular model potentials; namely SPC/E, TIP4P and TIP5P. Densities have been calculated for specific thermodynamic state points and compared to experimental results. The SPC/E and TIP4P models overestimate the solid densities by about 2%. The TIP5P model overestimates the solid densities by about 5–10%. The structural pair correlation functions between oxygen–oxygen, hydrogen–hydrogen and oxygen–hydrogen atoms were also obtained from the simulations. (These are available as ESI†). It has been found that SPC/E and TIP4P structural predictions are rather similar, with the only exception of ice II for which differences are visible between these two models. Predictions from the TIP5P are clearly different from those of the other models, especially for ices I_h and II. For the higher density ices structural differences between the models are rather small. Experimental data would be highly desirable to test the structural predictions of the different models of water. This is especially true for ice II. We have also found that the oxygen–oxygen correlation function of high density amorphous (HDA) water presents the same broad features as those exhibited by ice XII.

I. Introduction

The study of the phase diagram of water has a history spanning more than one hundred years.[1–4] With the rapid pace of scientific discovery in the 20th century this amounts to a testimony of the importance of this ubiquitous molecule. Today, thirteen solid phases of water are known, with the latest, ice XII, having been discovered by Lobban, Finney and Kuhs as recently as 1998.[5] Of these thirteen phases, nine are thermodynamically stable and four are metastable (I_c, IV, IX and XII).

For each of the solid phases, structural features such as the space group, unit cell parameters, and atomic positions have been investigated by means of X-ray or neutron diffraction studies. Atom–atom pair correlation functions for oxygen–oxygen (g_{OO}), oxygen–hydrogen (g_{OH}) and hydrogen–hydrogen (g_{HH}) are the principal structural descriptors for water. These diffraction studies are performed either under conditions for which the solid is thermodynamically stable, or at ambient pressure after quenching the solid in liquid nitrogen (77 K). Diffraction studies have also been performed for liquid water, leading to the total structure factor $S(k)$. In principle, a Fourier transform of the structure factor to real space leads to the aforementioned pair correlation functions. However, there are a number of stumbling blocks. Firstly, one requires a knowledge of the structure factor from $k = 0$ to $k = \infty$. Experimental data covers a wide but finite window of reciprocal space. The second problem is the teasing out of the three pair correlation functions from one total structure factor. One approach to this problem is the study of mixtures of D_2O with H_2O using neutron diffraction. An assumption with this method is that the substitution of hydrogen with its isotope does not affect the structure of water, which is not necessarily true.[6,7] There exist techniques for deriving large, three dimensional structures from the structure factors, such as 'reverse Monte Carlo'.[8–11] Soper has used the 'empirical potential structure refinement' (EPSR) simulation technique[12,13] to extract the experimental pair correlation functions using the ISIS SANDALS[14] neutron data for both liquid water and ice I_h.

With the development of the first electronic computing machines came the techniques of Monte Carlo[15–18] and Molecular Dynamics.[19] Both of these methods have been used to provide valuable insights into the behavior of liquids and solids at the molecular level. Computer simulations of water were soon to follow, with the pioneering papers of Barker and Watts[20] and of Rahman and Stillinger.[21] To date, thousands of simulation studies have been undertaken with water being either the principal component, or present as a mixture or solvent.[22–25]

One of the key features of simulation studies is the choice of model potential used to describe the molecular system in question. For water, a great many model potentials have been proposed over the years.[26] An excellent survey of such models has been presented in a review by Guillot.[27] Two of the most frequently encountered are the 'Simple Point Charge–Extended' model (SPC/E) of Berendsen *et al.*,[28] and the 'Four Point Transferable Intermolecular Potential' (TIP4P) of Jorgensen *et al.*[29] The more recent 'Five Point Transferable Intermolecular Potential' (TIP5P) of Mahoney and Jorgensen[30] is also receiving much interest. The parameters used in these models are often chosen to reproduce thermodynamic (density, energy, diffusion coefficient, dielectric constant, *etc.*) and/or structural properties[13,31] of water at room temperature and pressure. In view of this the oxygen–oxygen pair correlation function obtained from simulations of a given pair

potential is often used as the yard-stick against which model potentials are tested. The SPC/E and TIP4P models yield a fair description of the g_{OO} for liquid water at room temperature and pressure whilst TIP5P provides an excellent description of this function.

Somewhat surprisingly there is a paucity of computer studies of solid–fluid and solid–solid equilibria for water. The majority of studies that do treat the solid phase have mostly focused on ice I_h or I_c[32–39] with the notable exceptions of Baez and Clancy[40] (ices I, II, III, and IX), Ayala and Tchijov[41] (ice III and V), Borzsk and Cummings et al.[42] (ice XII) and the theoretical work by Woo and Monson[43] (ices I, II, and VI).

Recently, various authors have undertaken the task of determining the phase diagram of water for the SPC/E and TIP4P models.[44–47] Calculation of a phase diagram is a fairly involved process having a number of steps. Firstly, ideal crystal structures have to be created, not necessarily a trivial task. Then it is necessary to calculate the free energies for each of these ices. This was done using the Frenkel–Ladd method.[48,49] In some of the ice phases, namely ice III and ice V, the protons are partially disordered.[50] In order to calculate the entropy of such phases MacDowell et al.[46] extended the ideas of Howe and Whitworth.[51] Next, isobaric–isothermal (NpT) Monte Carlo simulations were performed using Parrinello–Rahman sampling[52] for both the fluid and the solid phases. These simulations were used to calculate the point for which both the chemical potential and the pressure were equal in each of the phases. Once a coexistence point had been determined for each of the phase transitions, the full coexistence lines were then traced out using the Gibbs–Duhem integration technique devised by Kofke.[53–57] The only ice excluded form this study was ice X (in ice X the protons lie in the middle point between contiguous oxygens of the lattice; this feature can not be mimicked by a model that has fixed bond lengths). One of the results of this study was to show that the TIP4P model does a good job of qualitatively describing the phase diagram of water.[44] A similar calculation for the phase diagram of the TIP5P model has so far not been undertaken, with the exception of the vapor–liquid equilibrium.[58]

This paper has two objectives. The first is to present the results for the density of various ice phases using the TIP5P model. These results are compared to the values provided by the TIP4P and SPC/E models. Secondly, the pair correlation functions are described for each of the models and for each of the phases, and are provided as ESI†. For many of the structures this is the first time that this information has been made available. Given this, until experimental results are presented it is difficult to say exactly which features for each of the models are the most salient.

In Section II the details of the simulation technique are given. In Section III the results of this work will be presented and in Section IV the main conclusions will be discussed.

II. Water models and simulation details

In Table 1 the geometry and the parameters for several popular potential models of water are presented. The TIP4P model was proposed by Jorgensen et al.[29] and is based upon a geometry originally suggested by Bernal and Fowler[59] in 1933. A single Lennard-Jones (LJ) interaction site is located at the position of the oxygen atom. Two positive point charges are located at the positions of the hydrogen atoms, and a negative charge is located on a point M which is placed at a distance d_{OM} from the oxygen along the H–O–H bisector in the direction of the positive charges. For the distances d_{OH} and the angle H–O–H, the TIP4P uses experimental values, whilst the remaining parameters were fitted to reproduce certain thermodynamic properties of liquid water. The SPC/E model, proposed in 1987 by Berendsen et al.[28] also consists of a LJ interaction site with a negative charge located at the position of the oxygen atom. Positive charges are placed on the hydrogen atoms (at a distance of 1 Å from the oxygen atom forming a tetrahedral angle). Berendsen et al. proposed that a polarization energy should be added to the internal energy of the liquid when fitting the potential parameters of the model to the vaporization enthalpy of real water. Finally, in 2000, Mahoney and Jorgensen[30] proposed a new potential model known as TIP5P. The geometry of TIP5P is similar to that of the water models of the nineteen seventies, such as ST2.[60] In addition to the LJ center located at the oxygen, and the partial charges located at the hydrogens, two partial charges are placed at the positions of the "lone electron pairs". Concerning computational cost, the SPC/E model requires the determination of 9 site–site distances, TIP4P needs 10 (9 charge–charge distances and the LJ interaction) and the TIP5P requires 17 (16 charge–charge distances plus the LJ interaction). Therefore, computer time for these models scales approximately as 9 to 10 to 17, respectively.

It should be mentioned that all these models are pair-wise additive, and simplify the true interaction between water molecules i.e. they neglect molecular flexibility, polarizability, quantum effects, etc. and were parameterized using a spherical cut-off (i.e. without recourse to either reaction fields or Ewald sums). However, due to their simplicity they are the most popular water models encountered in computer simulation studies.

In the simulations described in this work the LJ potential was truncated at 8.5 Å for all of the phases. Standard long range corrections to the LJ energy were added. The importance of an adequate treatment of the long range Coulombic forces when dealing with water simulations has been pointed out in recent studies.[61–63] In this work, the Ewald summation technique, along with a linked cell list (described in ref. 64) has been employed for the calculation of the long range electrostatic forces. The screening parameter and the number of vectors of reciprocal space considered had to be carefully selected for each crystal phase.[65,66] The number of molecules for each phase was chosen so as to fit at least twice the cutoff distance in each direction. This varied between ≈ 300 and ≈ 600 molecules, depending on the particular solid structure. NpT Monte Carlo simulations were performed for the above mentioned water models. Isotropic changes in the volume of the simulation box are adequate for the liquid phase, while anisotropic Monte Carlo simulations (Parrinello–Rahman like[52,67])

Table 1 Parameters used to describe the potentials for the water models used in this work. The distance between the oxygen and hydrogen sites is d_{OH}. The angle formed by the hydrogen, oxygen and the remaining hydrogen atom is denoted as H–O–H. The LJ site is located on the oxygen with parameters σ and ε/k. The charge on the proton is q_H. The SPC/E and TIP4P models place the negative charge at a point M at a distance d_{OM} from the oxygen along the H–O–H bisector. For TIP5P, d_{OL} is the distance between the oxygen and the sites L placed at the "lone electron pairs" (the angle L–O–L is the tetrahedral angle 109.47)

Model	d_{OH}/Å	H–O–H	σ/Å	(ε/k)/K	q_H/e	d_{OM}/Å	d_{OL}/Å	Ref.
SPC/E	1.0	109.47	3.1656	78.20	0.4238	0	—	28
TIP4P	0.9572	104.52	3.1540	78.02	0.52	0.15	—	29
TIP5P	0.9572	104.52	3.1200	80.51	0.241	—	0.70	30

Table 2 Densities and residual internal energies of water ice phases considered in this work as obtained from NpT simulations for the TIP4P, SPC/E and TIP5P models. Experimental data for the ices are taken from ref. 72, except that of ice VII, taken from ref. 85

| Phase | T/K | p/GPa | ρ/g cm^{-3} | | | | U/kcal mol^{-1} | | |
			Exptl.	TIP4P	SPC/E	TIP5P	TIP4P	SPC/E	TIP5P
Liquid	300	10^{-4}	0.996	0.994	1.000	0.982	−9.87	−11.15	−9.66
I$_h$	250	0	0.920	0.937	0.944	0.976	−11.89	−12.93	−12.31
I$_h$^{b}	250	0	0.920		0.947				
I$_c$	78	0	0.931	0.964	0.971	1.026	−13.15	−14.22	−13.66
II	123	0	1.170	1.220	1.245	1.284	−12.61	−14.08	−13.37
III	250	0.28	1.165	1.175	1.171	1.185	−11.58	−12.62	−11.49
III	250	0.25		1.170		1.181	−11.58		−11.48
III^c	250	0.25		1.175		1.203			
IV	110	0	1.272	1.314	1.324^a	1.371	−12.29	−13.29^a	−12.33
V	223	0.53	1.283	1.294	1.294	1.331	−11.75	−12.71	−11.60
V	250	0.5		1.280		1.316	−11.52		−11.38
V^c	250	0.5		1.276		1.319			
VI	225	1.1	1.373	1.406	1.403	1.447	−11.65	−12.53	−11.42
VII	300	10	1.880	1.832	1.822	1.895	−8.56	−9.42	−8.916
VIII	10	2.4	1.628	1.674	1.679	1.760	−11.47	−12.31	−11.49
IX	165	0.28	1.194	1.210	1.219	1.231	−12.49	−13.70	−12.71
XII	260	0.5	1.292	1.314	1.313	1.340	−11.35	−12.29	−11.06
XI	5	0	0.934	0.976	0.985	1.046	−13.61	−14.73	−14.22

^{a} Note that these results marked (ice IV) were mis-printed in ref. 44. Results from other authors have been included in the Table: ^{b} from Gay et al.[74] ^{c} from Ayala and Tchijov.[41]

were necessary for the solid phases, thus allowing both the shape and the relative dimensions of the unit cell to change. Typically, about 40 000 cycles were undertaken for the determination the properties of each phase for a given state (a cycle is defined as a trial move per particle plus a trial volume change). These properties were calculated after a 40 000 cycle equilibration period. For the disordered phases (I$_h$, I$_c$, IV, VI, VII, XII) the algorithm of Buch et al.[68] was used to generate an initial configuration having no net dipole moment where the hydrogens (but not the oxygens) are disordered and satisfy the ice rules.[59,69] The remaining disordered phases, ice III and ice V, required some additional care, as they are known to exhibit only partial disorder.[50] In view of this the algorithm given in ref. 68 was generalized[46] in order to generate an initial configuration with biased occupation of the hydrogen positions. Ice II, VIII and IX are proton ordered, thus crystallographic information was used to generate an initial solid configuration.[70] For ice XI the antiferroelectric structure of ice I$_h$[71] was used.

The atom–atom correlation functions were evaluated every 5 cycles. The width of the grid used to compute $g(r)$ was of the order of 0.05 Å. Correlation functions were evaluated up to 7.5 Å.

III. Results

A. Solid densities

In Table 2 the density for each of the phases considered in this work is presented alongside experimental results. The thermodynamic state points considered were chosen to coincide with those given in Table 11.2 of the book by Petrenko and Whitworth.[72] Results for the SPC/E and TIP4P models have been taken from ref. 44. As can be seen, although the solid densities of SPC/E and TIP4P models are quite similar and compare rather well with the experimental results (overestimating the solid densities by about $\approx 2\%$), the TIP5P overestimates the experimental densities by ≈ 5–10%. Thus the TIP5P model is not the most suitable model for the description of the equation of state of ice phases (in a different study[73] it has also been found that the TIP5P has difficulty in reproducing the relative stability between ice I$_h$ and ice II). Table 2 also presents simulation results from other groups. Good agreement has been found for the density of ice I$_h$ as reported by Haymet et al.[74] as well as for Tchijov et al.[41] for ices III and V.

The Parrinello–Rahman implementation of the isobaric isothermal ensemble allows the geometry of the simulation box (a, b, c, α, β and γ) to fluctuate during the simulation. This

Table 3 Densities and unit cell parameters of the ice phases considered in this work. The experimental data are taken from ref. 72, except that of ice VII, taken from ref. 85. Lengths are given in Å. Simulation results are for the TIP4P model

| Phase | T/K | p/GPa | ρ/g cm^{-3} | | Unit cell | |
			Exptl.	Simulation	Exptl.	Simulation
I$_h$	250	0	0.920	0.937	$a = 4.518, c = 7.356$	$a = 4.490, c = 7.318$
I$_c$	78	0	0.931	0.964	$a = 6.358$	$a = 6.284$
II	123	0	1.170	1.220	$a = 7.78, \alpha = 113.1°$	$a = 7.690, \alpha = 113.1°$
III	250	0.28	1.165	1.175	$a = 6.666, c = 6.936$	$a = 6.609, c = 6.997$
IV	110	0	1.272	1.314	$a = 7.60, \alpha = 70.1°$	$a = 7.530 \, \alpha = 69.93°$
V	223	0.53	1.283	1.294		
VI	225	1.1	1.373	1.406	$a = 6.181, c = 5.698$	$a = 6.124, c = 5.673$
VII	300	10	1.880	1.832	$a = 3.169$	$a = 3.196$
VIII	10	2.4	1.628	1.674	$a = 4.656, c = 6.775$	$a = 4.538, c = 6.940$
IX	165	0.28	1.194	1.210	$a = 6.692, c = 6.715$	$a = 6.634, c = 6.739$
XII	260	0.5	1.292	1.314	$a = 8.304, c = 4.024$	$a = 8.279, c = 3.986$
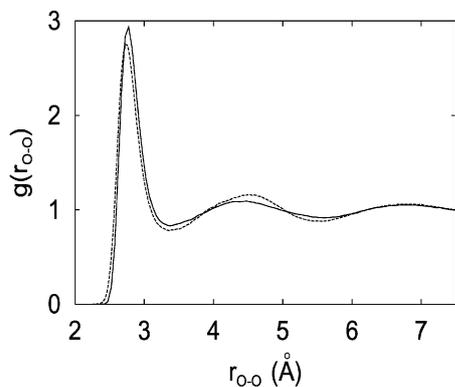
Fig. 1 Comparison between TIP4P water at 300 K (solid line) and Soper water at 298 K and 0.1 MPa (dashed line).

Fig. 3 Oxygen–oxygen site–site distribution function for ice I_h at 250 K and 0 GPa. TIP4P solid line, TIP5P dashed line and SPC/E dotted line.

leads directly to the geometry of the crystallographic unit cell. In Table 3 a, b, c, α, β and γ are given for each of the phases for the TIP4P model. As can be seen the agreement with experiment is quite good.

B. Liquid water

In this section a comparison is made between the structural results of the liquid phase for the both the TIP4P (Fig. 1) and the TIP5P (Fig. 2) models at $T = 300$ K and $p = 0.1$ MPa alongside the experimental results of Soper at $T = 298$ K and $p = 0.1$ MPa.[13] Both the TIP4P and TIP5P models provide a very good description of the experimental g_{OO}. This is no surprise, given that the parameters of both of these models were designed to reproduce the density, enthalpy of vaporization and structure of liquid water. The simulation results presented here are in agreement with previously published results and provide a rough cross check of the simulation methodology employed in this work. It should be noted, however, that in a large number of studies the pair potential was truncated and Ewald sums were not used.

C. Ice phases

Let us now proceed to the structural results for the solid phases. The thermodynamic states studied were chosen to coincide with the state points given in Table 11.2 of the book by Petrenko and Whitworth.[72] In Fig. 3 g_{OO} is plotted for ice I_h for each of the three models (SPC/E, TIP4P and TIP5P). The structure for both the SPC/E and TIP4P models is very similar, while the structure for TIP5P is somewhat different. For the ice I_h phase we are fortunate in having the experimental data of Soper to compare with.[13] In Fig. 4 the experimental data is compared to the TIP4P model, and in Fig. 5 to the TIP5P

model. The TIP4P and TIP5P models perform well when reproducing the location of the second and fourth peaks seen in the experimental g_{OO}. None of the potential models reproduce the first (seen at 2.43 Å) and third (seen at 3.48 Å) peaks present in the experimental data. Both the TIP4P and the TIP5P models overestimate the height of the second experimental peak. It is interesting to speculate whether the addition of the small experimental (somewhat unusual) first peak with the much larger second peak would place the simulation results in a more favorable light. Qualitative differences are also found when considering the structure at a distance of about 5.3 Å. While the SPC/E and TIP4P models show a slight shoulder, the TIP5P model presents a third peak, corresponding to the fifth peak at 5.46 Å in the experimental data.

We shall now move on to the structure of ice II (Fig. 6). Overall the g_{OO} produced by the SPC/E and TIP4P models is similar, although for ice II (in contrast to ice I_h) slight differences are noticeable. The most striking differences start at $r \approx 4.2$ Å, where one sees a deep minimum for the TIP5P model, a plateau for the TIP4P model, and a small peak for the SPC/E model. Obviously only experimental results could decide which (if any) correctly reproduces the true inter-atomic structure.

A feature of ice II, which it shares with ices VIII, IX and XI, is that it has an ordered proton structure. In all the other ice phases the hydrogens are either completely disordered, or show only partial ordering. The density of ice II is $\approx 30\%$ larger than that of ice I_h. The origin of this difference is clearly illustrated by comparing g_{OO} for ice I_h (Fig. 3) against that of ice II (Fig. 6). The second peak for ice I_h is located at 4.53 Å, whereas for ice II it shifts to 3.53 Å. The reduced radius of this second coordination layer leads to the higher packing efficiency of ice II (at the cost of forming a distorted tetrahedral configuration in the first coordination layer).

Fig. 2 Comparison between TIP5P water at 300 K (solid line) and Soper water at 298 K and 0.1 MPa (dashed line).
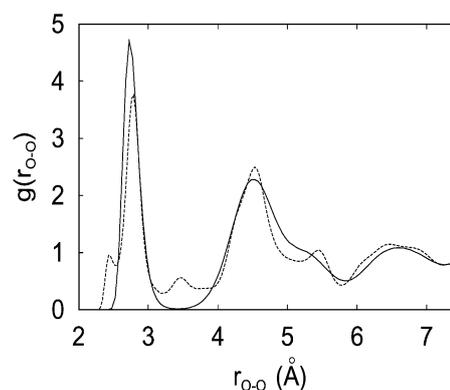
Fig. 4 Comparison between TIP4P ice I_h at 250 K and $p = 0$ (solid line) and Soper ice at 220 K and $p = 0.1$ MPa (dashed line).
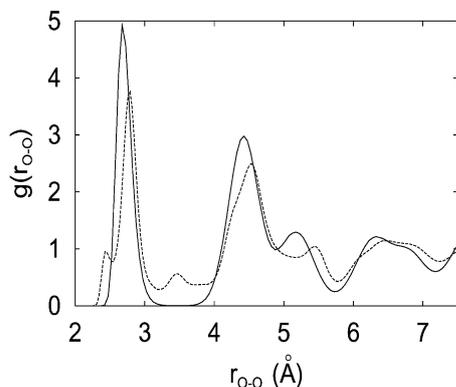
Fig. 5 Comparison between TIP5P ice I_h at 250 K and $p = 0$ (solid line) and Soper ice at 220 K and $p = 0.1$ MPa (dashed line).

Moving to higher densities one encounters ices III, V and VI. Ice III and V achieve this higher density in a similar fashion to ice II; by distorting its tetrahedral configuration. Ice VI goes one step further, by forming not one but two distinct inter-penetrated hydrogen bonded networks.

For ice III the g_{OO} of the SPC/E and TIP4P models are once again almost indistinguishable (Fig. 7). The TIP5P structure is also very similar, however, the second and third peaks are slightly higher. It is interesting to note that, whilst the TIP5P showed significant differences with the other models for ice II, these differences are considerably smaller for ice III. The increase in temperature is probably a contributing factor. However, one possibly key factor is the proton disorder present in ice III. Apparently the proton order of ice II contributes significantly to the structural differences found for ice II for the three potential models.

In Figs. 8 and 9 the g_{OO} for ices V and VI are presented. In a similar manner to ice III, each of the models are very similar, with TIP5P showing the greatest differences. We conclude that for hydrogen disordered ices, structural differences between g_{OO} of different models tend to decrease as the density of the ice phase increases. With a view to improving the quality of future models of water, experimental data for the atom–atom correlation functions of ices I_h and II would be the most useful, given the insensitivity seen in ices III, V and VI.

Let us finally consider the high density ices, namely ice VII and ice VIII. Both solids present two-inter penetrating, but not interconnected, hydrogen bonded networks. In ice VII, the hydrogens are disordered whereas in ice VIII they are ordered. In Fig. 10 the results for ice VII are presented. Differences between the potential models are small. If one imagines the ice VIII–ice VII transition to be an order–disorder transition (in fact the location of the oxygens is quite similar and the main difference is the order–disordered configuration of the hydro-

Fig. 7 Oxygen–oxygen site–site distribution function for ice III at 250 K and 0.28 GPa. TIP4P solid line, TIP5P dashed line and SPC/E dotted line.
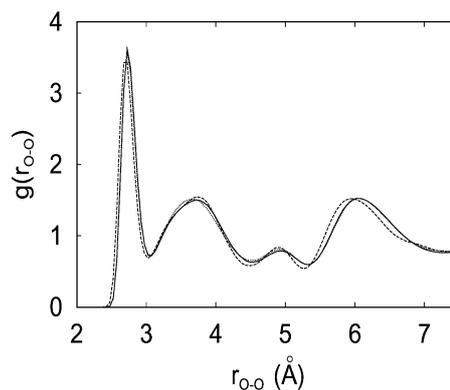
Fig. 8 Oxygen–oxygen site–site distribution function for ice V at 223 K and 0.53 GPa. TIP4P solid line, TIP5P dashed line and SPC/E dotted line.

gens) then it is possible to see the ice VII g_{OO} structure splitting up into doublets to accommodate this change. This splitting is provoked by the change in symmetry from cubic (ice VII) to tetragonal (ice VIII). This is presented in Fig. 11. The coordination number of the nearest neighbors is 8 for these two structures.

D. HDA

Since the pioneering work of Mishima et al.,[75] high density amorphous water (HDA) has been the focus of a number of studies, (not least because of the possible existence of a liquid–liquid critical point[76,77]). Mishima showed that when ice I_h is compressed at 77 K, amorphous water is formed at about

Fig. 6 Oxygen–oxygen site–site distribution function for ice II at 123 K and 0 GPa. TIP4P solid line, TIP5P dashed line and SPC/E dotted line.
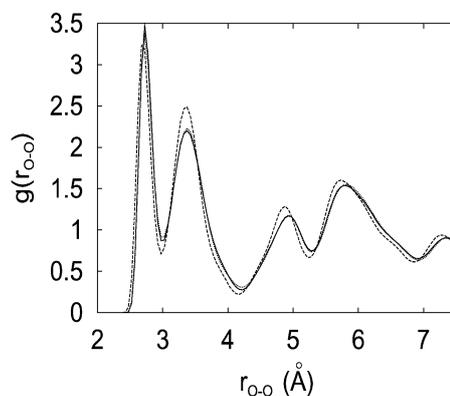
Fig. 9 Oxygen–oxygen site–site distribution function for ice VI at 225 K and 1.1 GPa. TIP4P solid line, TIP5P dashed line and SPC/E dotted line.
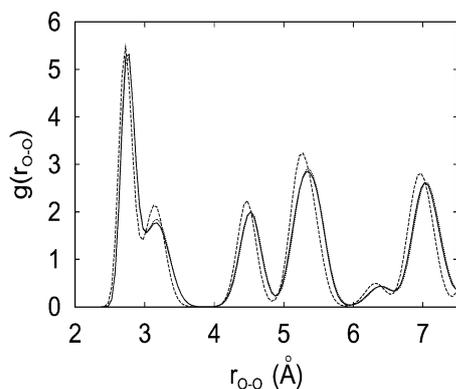
Fig. 10 Oxygen–oxygen site–site distribution function for ice VII at 300 K and 10 GPa. TIP4P solid line, TIP5P dashed line and SPC/E dotted line.

Fig. 12 Comparison between TIP4P ice XII (dashed line) at 77 K and a HDA phase at 77 K, both at 1.7 GPa (solid line).

1.5 GPa. Later simulation studies by Tse and Klein,[78] also reproduced this amorphization process. It has recently been shown using computer simulation that HDA can not only be obtained from I_h, but also from ice VII and ice VIII, provided that the melting line of the model is crossed.[79] The properties of HDA have been determined experimentally by a number of groups. A surprising result was obtained a few years ago by Koza et al.[80] showing that when compressing ice I_h at 77 K, it was possible to form ice XII. It was initially thought that ice I_h transformed directly into ice XII. However, it is now known that HDA acts as an intermediate step[81] so that the sequence is I_h, HDA, ice XII. It has been suggested that a shock wave is capable of generating transient local heating provoking a HDA–ice XII transition.[81] One structural detail that goes some way to explain the preference for the formation of ice XII is the fact that this ice is the only one that has 'rings' of 7 and 8 oxygen atoms.[82] It has also been shown that HDA has rings of 7, 8 and even 9 oxygen atoms.[83,84] In Fig. 12 the g_{OO} for HDA and for ice XII at $T = 77$ K and 1.7 GPa are shown. The HDA phase was obtained by amorphization of ice I_h at $T = 77$ K as described in ref. 79. As can be seen, the location of the peaks for the ice XII phase show a rough correspondence with the structure of the HDA. Obviously this is only an inference, given the great difference between a crystalline solid with long range order, and a amorphous structure having only short range structure. It is also interesting to note the similarity in densities of these two phases; HDA having $\rho = 1.38$ and ice XII $\rho = 1.44$ (g cm^{-3}).

At present there is no theory to allow the prediction of the activation energy associated with an amorphous to crystalline solid transition. This would be an interesting task for a density functional theory.
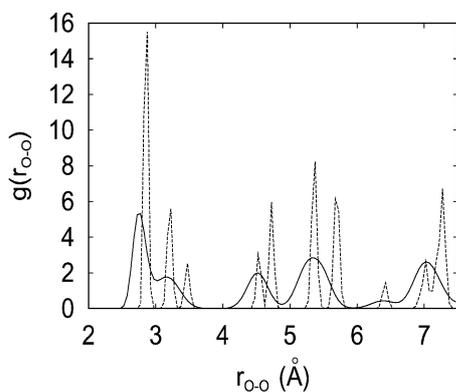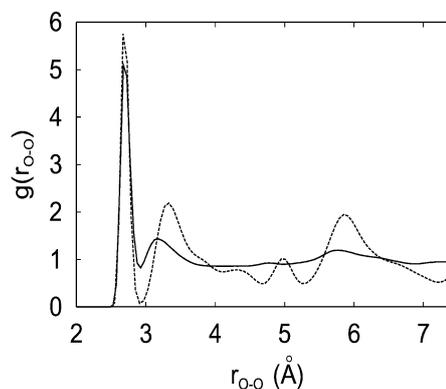
IV. Conclusion

In this paper the atom–atom correlation functions, g_{OO}, g_{OH} and g_{HH} have been determined for practically all of the solid phases of water using computer simulation. All of these functions are available electronically via ESI† . Three models were considered; SPC/E, TIP4P and TIP5P. The SPC/E and TIP4P models do a good job in describing the density of the different ice phases, overestimating the experimental densities by $\approx 2\%$. The TIP5P does not fare so well, overestimating the density of the different solid phases by about 5–10%. In view of this we conclude that the SPC/E and TIP4P are more suitable for deriving the equations of state for the ice phases.

The SPC/E and TIP4P models also yield rather similar structural predictions for most ice phases, with the only exception being ice II, for which differences between SPC/E and TIP4P are clearly visible. The structural predictions of the TIP5P model differ significantly from those of the two other potential models, especially with respect to ices I_h and II. As the density of the ice phases increases (i.e. ice III, V and VI) the differences between the SPC/E, TIP4P and TIP5P models tend to become smaller.

It is difficult to assess exactly which features in each of the models leads to a better or worse description of the structure of the ice phases. This is due greatly in part to the dearth of experimental studies for all of the ices apart from ice I_h. More structural experimental results on ices would be highly desirable. Even with the experimental atom–atom pair correlation functions there exist structural features not seen in the computational studies (such as the first peak at 2.43 Å and the third peak at 3.48 Å seen in the experimental ice I_h data at 220 K).

We have also studied the g_{OO} for the high density amorphous phase of water (HDA). Given that ice I_h transforms into ice XII, via the formation of HDA,[81] the structure of these two phases has also been analyzed. We have found, that, although a strong structural similarity between a solid and an amorphous phase obviously does not exist, the broad features of the g_{OO} exhibited by HDA are similar to those of ice XII when compared under the same conditions. The height and location of the first peak and the trends seen in the rest of the curve share a certain similarity. It would be quite interesting to develop a theoretical approach to understand the formation of ice XII from HDA, along with a mechanism and activation energy of such a process.

Fig. 11 Comparison between ice VII (solid line) at 300 K and 10 GPa, and ice VIII (dashed line) at 10 K and 2.4 GPa.

References

1 G. Tammann, *Ann. Phys.*, 1900, **2**, 1.
2 P. W. Bridgman, *Proc. Am. Acad. Arts Sci.*, 1912, **XLVII**, 441.
3 P. W. Bridgman, *J. Chem. Phys.*, 1935, **3**, 597.
4 P. W. Bridgman, *J. Chem. Phys.*, 1937, **5**, 964.
5 C. Lobban, J. L. Finney and W. F. Kuhs, *Nature*, 1998, **391**, 268.
6 J. H. Root, P. A. Egelstaff and A. Hime, *Chem. Phys.*, 1986, **109**, 437.
7 R. A. Kuharski and P. J. Rossky, *J. Chem. Phys.*, 1985, **83**, 5164.
8 R. L. McGreevy and L. Pusztai, *Mol. Simul.*, 1988, **1**, 359.
9 R. L. McGreevy and M. A. Howe, *Annu. Rev. Mater. Sci.*, 1992, **22**, 217.
10 R. L. McGreevy, *Nucl. Instrum. Methods, Sect. A*, 1995, **354**, 1.
11 P. Jóvári and L. Pusztai, in *New Kinds of Phase Transitions: Transformation in Disordered Substances, Vol. 81 of NATO Science Series II: Mathematics Physics and Chemistry*, Kluwer Academic Publishers, 2002, vol. 81, p. 267.
12 A. K. Soper, *J. Mol. Liq.*, 1998, **78**, 179.
13 A. K. Soper, *Chem. Phys.*, 2000, **258**, 121.
14 http://www.isis.rl.ac.uk/disordered/Database.
15 N. Metropolis and S. Ulam, *J. Am. Stat. Assoc.*, 1949, **44**, 335.
16 N. Metropolis, *Los Alamos Science*, 1987, **15**, 125.
17 N. Metropolis, A. W. Rosenbluth, M. N. Rosenbluth, A. H. Teller and E. Teller, *J. Chem. Phys.*, 1953, **21**, 1087.
18 B. J. Alder and T. E. Wainwright, *J. Chem. Phys.*, 1957, **27**, 1208.
19 B. J. Alder and T. E. Wainwright, *J. Chem. Phys.*, 1959, **31**, 459.
20 J. A. Barker and R. O. Watts, *Chem. Phys. Lett.*, 1969, **3**, 144.
21 A. Rahman and F. H. Stillinger, *J. Chem. Phys.*, 1971, **55**, 3336.
22 R. Lynden-Bell, J. Rasaiah and J. Noworyta, *Pure Appl. Chem.*, 2001, **73**, 1721.
23 K. M. Åberg, A. P. Lyubartsev, S. P. Jacobsson and A. Laaksonen, *J. Chem. Phys.*, 2004, **120**, 3770.
24 M. Ferrario, G. Ciccotti, E. Spohr, T. Cartailler and P. Turq, *J. Chem. Phys.*, 2002, **117**, 4947.
25 D. Paschek, *J. Chem. Phys.*, 2004, **120**, 6674.
26 J. L. Finney, J. E. Quinn and J. O. Baum, in *Water Science Reviews 1*, ed. F. Franks, Cambridge University Press, Cambridge, 1985.
27 B. Guillot, *J. Mol. Liq.*, 2002, **101**, 219.
28 H. J. C. Berendsen, J. R. Grigera and T. P. Straatsma, *J. Phys. Chem.*, 1987, **91**, 6269.
29 W. L. Jorgensen, J. Chandrasekhar, J. D. Madura, R. W. Impey and M. L. Klein, *J. Chem. Phys.*, 1983, **79**, 926.
30 M. W. Mahoney and W. L. Jorgensen, *J. Chem. Phys.*, 2000, **112**, 8910.
31 T. Head-Gordon and G. Hura, *Chem. Rev.*, 2002, **102**, 2651.
32 G. T. Gao, X. C. Zeng and H. Tanaka, *J. Chem. Phys.*, 2000, **112**, 8534.
33 M. J. Vlot, J. Huinink and J. P. van der Eerden, *J. Chem. Phys.*, 1999, **110**, 55.
34 H. Nada and J. P. J. M. van der Eerden, *J. Chem. Phys.*, 2003, **118**, 7401.
35 B. W. Arbuckle and P. Clancy, *J. Chem. Phys.*, 2002, **116**, 5090.
36 T. Bryk and A. D. J. Haymet, *J. Chem. Phys.*, 2002, **117**, 10258.
37 T. Bryk and A. Haymet, *Mol. Simul.*, 2004, **30**, 131.
38 M. D. Morse and S. A. Rice, *J. Chem. Phys.*, 1982, **76**, 650.
39 S. W. Rick and A. D. J. Haymet, *J. Chem. Phys.*, 2003, **118**, 9291.
40 L. A. Báez and P. Clancy, *J. Chem. Phys.*, 1995, **103**, 9744.
41 R. B. Ayala and V. Tchijov, *Can. J. Phys.*, 2003, **81**, 11.
42 I. Borzsk and P. T. Cummings, *Chem. Phys. Lett.*, 1999, **300**, 359.
43 H.-J. Woo and P. A. Monson, *J. Chem. Phys.*, 2003, **118**, 7005.
44 E. Sanz, C. Vega, J. L. F. Abascal and L. G. MacDowell, *Phys. Rev. Lett.*, 2004, **92**, 255701.
45 E. Sanz, C. Vega, J. L. F. Abascal and L. G. MacDowell, *J. Chem. Phys.*, 2004, **121**, 1165.
46 L. G. MacDowell, E. Sanz, C. Vega and J. L. F. Abascal, *J. Chem. Phys.*, 2004, **121**, 10145.
47 C. McBride, C. Vega, E. Sanz, L. G. MacDowell and J. L. F. Abascal, *Mol. Phys.*, 2005, **103**, 1.
48 D. Frenkel and A. J. C. Ladd, *J. Chem. Phys.*, 1984, **81**, 3188.
49 C. Vega and P. A. Monson, *J. Chem. Phys.*, 1998, **109**, 9938.
50 C. Lobban, J. L. Finney and W. F. Kuhs, *J. Chem. Phys.*, 2000, **112**, 7169.
51 R. Howe and R. W. Whitworth, *J. Chem. Phys.*, 1987, **86**, 6443.
52 M. Parrinello and A. Rahman, *J. Appl. Phys.*, 1981, **52**, 7182.
53 D. A. Kofke, *J. Chem. Phys.*, 1993, **98**, 4149.
54 D. A. Kofke, *Mol. Phys.*, 1993, **78**, 1331.
55 R. Agrawal and D. A. Kofke, *Mol. Phys.*, 1995, **85**, 43.
56 D. A. Kofke, in *Monte Carlo Methods in Chemical Physics*, ed. D. M. Ferguson, J. I. Siepmann and D. G. Truhlar, John Wiley and Sons, 1998, vol. 105, p. 405.
57 P. A. Monson and D. A. Kofke, in *Advances in Chemical Physics*, ed. I. Prigogine and S. A. Rice, John Wiley and Sons, 2000, vol. 115, p. 113.
58 M. Lísal, I. Nezbeda and W. R. Smith, *J. Phys. Chem. B*, 2004, **108**, 7412.
59 J. D. Bernal and R. H. Fowler, *J. Chem. Phys.*, 1933, **1**, 515.
60 F. H. Stillinger and A. Rahman, *J. Chem. Phys.*, 1974, **60**, 1545.
61 D. van der Spoel, P. J. van Maaren and H. J. C. Berendsen, *J. Chem. Phys.*, 1998, **108**, 10220.
62 M. Lísal, J. Kolafa and I. Nezbeda, *J. Chem. Phys.*, 2002, **117**, 8892.
63 S. W. Rick, *J. Chem. Phys.*, 2004, **120**, 6085.
64 L. G. MacDowell, *Termodinámica Estadística de Moléculas Flexibles: Teoría y Simulación*, PhD Thesis, Universidad Complutense de Madrid, Facultad de C.C. Químicas, 2000.
65 M. P. Allen and D. J. Tildesley, *Computer Simulation of Liquids*, Oxford University Press, 1987.
66 D. Frenkel and B. Smit, *Understanding Molecular Simulation*, Academic Press, London, 1996.
67 S. Yashonath and C. N. R. Rao, *Mol. Phys.*, 1985, **54**, 245.
68 V. Buch, P. Sandler and J. Sadlej, *J. Phys. Chem. B*, 1998, **102**, 8641.
69 L. Pauling, *J. Am. Chem. Soc.*, 1935, **57**, 2680.
70 C. Lobban, J. L. Finney and W. F. Kuhs, *J. Chem. Phys.*, 2002, **117**, 3928.
71 E. R. Davidson and K. Morokuma, *J. Chem. Phys.*, 1984, **81**, 3741.
72 V. F. Petrenko and R. W. Whitworth, *Physics of Ice*, Oxford University Press, 1999.
73 C. Vega, E. Sanz and J. L. F. Abascal, *J. Chem. Phys.*, 2005, in press.
74 S. C. Gay, E. J. Smith and A. D. J. Haymet, *J. Chem. Phys.*, 2002, **116**, 8876.
75 O. Mishima, L. D. Calvert and E. Whalley, *Nature*, 1984, **310**, 393.
76 P. H. Poole, F. Sciortino, U. Essmann and H. E. Stanley, *Nature*, 1992, **360**, 324.
77 P. H. Poole, U. Essmann, F. Sciortino and H. E. Stanley, *Phys. Rev. E*, 1993, **48**, 4605.
78 J. S. Tse and M. L. Klein, *Phys. Rev. Lett.*, 1987, **58**, 1672.
79 C. McBride, C. Vega, E. Sanz and J. L. F. Abascal, *J. Chem. Phys.*, 2004, **121**, 11907.
80 M. M. Koza, H. Schober, T. Hansen, A. Tlle and F. Fujara, *Phys. Rev. Lett.*, 2000, **84**, 4112.
81 I. Kohl, E. Mayer and A. Hallbrucker, *Phys. Chem. Chem. Phys.*, 2001, **3**, 602.
82 M. O'Keeffe, *Nature*, 1998, **382**, 879.
83 R. Martoňáak, D. Donadio and M. Parrinello, *Phys. Rev. Lett.*, 2004, **92**, 225702.
84 R. Martonak, D. Donadio and M. Parrinello, Topological defects and bulk melting of hexagonal ice, *arXiv*, 2005, **cond–mat**, 501543,http://arxiv.org/abs/cond-mat/0502042.
85 R. J. Hemley, A. P. Jephcoat, H. K. Mao, C. S. Zha, L. W. Finger and D. E. Cox, *Nature*, 1987, **330**, 737.